Glucosylated free oligosaccharides are biomarkers of endoplasmic reticulum alpha-glucosidase inhibition

Dominic S Alonzi, David Ca Neville, Robin H Lachmann, Raymond A Dwek, Terry D Butters

Glucosylated Free Oligosaccharides are Biomarkers of Endoplasmic Reticulum α-Glucosidase Inhibition

Dominic S. Alonzi[†], David C.A. Neville[†], Robin H. Lachmann[§], Raymond A. Dwek[†] and Terry D. Butters[†]

[†]Oxford Glycobiology Institute, Department of Biochemistry, University of Oxford, South Parks Road, Oxford OX1 3QU, UK

[§]Department of Medicine, University of Cambridge, Cambridge CB2 2QQ

Running Title: Glucosidase inhibition in vivo

Key Words: deoxynojirimycin, glycoprotein, degradation, renal excretion

Address correspondence to: Terry D. Butters, Oxford Glycobiology Institute, Department of Biochemistry, University of Oxford, South Parks Road, Oxford OX1 3QU, UK, Tel. +44 (0)1865 275725; Fax. +44 (0)1865 275216; E-Mail; terry.butters@bioch.ox.ac.uk

ABSTRACT

The inhibition of endoplasmic reticulum (ER) α-glucosidases I and II by imino sugars including *N*-butyl-deoxynojirimycin (*N*B-DNJ), causes the retention of glucose residues on N-linked oligosaccharides. Therefore, normal glycoprotein trafficking and processing through the glycosylation pathway is abrogated and glycoproteins are directed to undergo ER-associated degradation (ERAD), a consequence of which is the production of cytosolic free oligosaccharides (FOS). Following treatment with *N*B-DNJ, FOS were extracted from cells, murine tissues and human plasma and urine. Improved protocols for analysis were developed using ion-exchange chromatography followed by fluorescent labelling with 2-AA (anthranilic acid) and purification by lectin-affinity chromatography. Separation of 2-AA-labelled FOS by HPLC provided a rapid and sensitive method that enabled the detection of all FOS species resulting from the degradation of glycoproteins exported from the ER. The generation of oligosaccharides derived from glucosylated protein degradation was rapid, reversible, and time and inhibitor concentration dependent in cultured cells and *in vivo*. Long-term inhibition in cultured cells and *in vivo* indicated a slow rate of clearance of glucosylated free oligosaccharides. In mouse and human urine, glucosylated free oligosaccharides were detected as a result of transrenal excretion and provide unique and quantifiable biomarkers of ER-glucosidase inhibition.

INTRODUCTION

The N-alkylated glucose analogue, *N*-butyl-deoxynojirimycin (*N*B-DNJ) [1,2-4], is an inhibitor of both N-glycan processing enzymes of the ER, α-glucosidases I and II, and ceramide-specific glucosyltransferase, a key enzyme in the glycolipid biosynthetic pathway [5, 6]. *N*B-DNJ has been developed as an effective treatment, known as 'substrate reduction therapy' (SRT), for lysosomal storage diseases, in particular type I Gaucher disease for which clinical trials have been undertaken [7]. *N*B-DNJ (miglustat, Zavesca®) is now an approved medicine in the USA, Europe and Israel for this disorder. Clinically, a partial inhibition of the ceramide-specific glucosyltransferase by *N*B-DNJ is required to reduce glycolipid substrate synthesis at doses where side effects, such as glucosidase inhibition, are minimised. However, glucosidase inhibition also has therapeutic utility in reducing viral infectivity. Disruption of N-linked oligosaccharide processing by imino sugar-mediated ER glucosidase inhibition perturbs virus-sensitive protein-folding pathways in the cell [8, 9].

Imino sugars quickly and efficiently cross the plasma membrane such that the concentration of imino sugars in the cytosol is at equilibrium with the extracellular concentration [2]. In the cytosol imino sugars interact directly with the ceramide-specific glucosyltransferase on the cytosolic side of the *cis*-Golgi inhibiting glycolipid biosynthesis. However, to modulate N-linked processing by glucosidase inhibition imino sugars have to gain entry to the ER lumen. The rate of entry into the ER is unknown but the concentration of imino sugar is assumed to be much lower in the ER lumen than is supplied exogenously to the cell. Evidence for this comes from cellular experiments where the concentration of N-alkylated DNJ-based imino sugars required to inhibit ER glucosidase I has been measured, often requiring 1,000-10,000 times that which inhibits the purified enzyme *in vitro* [10].

Following access to the lumen of the ER, DNJ and its alkylated analogues inhibit the removal of glucose residues mediated by α-glucosidases I and II. This results in a large increase in the amount of glucosylated high-mannose containing oligosaccharides present on glycoproteins that are unable to utilise

the calnexin-(CNX) and calreticulin-(CRT) mediated folding pathways. These misfolded glycoproteins enter the ER associated degradation (ERAD) pathway for subsequent removal of the oligosaccharide and protein degradation. Therefore, an increase in glucosylated FOS in the presence of glucosidase inhibitors is observed in the cell [3]. Glucosylated FOS may also be produced as a result of the release of $Glc_3Man_9GlcNAc_2$ by ER-oligosaccharyltransferase (OST)-mediated hydrolysis of the dolichol precursor [11] which serves to control the size of the lipid-linked pool. Previous work has examined the relative level of FOS production by these separate pathways using virus infected, or non-infected cells treated with glycosidase inhibitors and has shown that the FOS produced are almost exclusively protein derived [12] (Alonzi et al., unpublished).

The removal of misfolded protein from the ER and production of free oligosaccharides (FOS) is a normal cellular process. Calnexin- or calreticulin-dependent, aberrantly-folded protein and hyperglucosylated, aberrantly-folded proteins are ultimately translocated out of the ER into the cytosol via the Sec61p channel [13]. The N-linked oligosaccharide is subsequently released by a cytosolic peptide:N-glycanase (PNGase) (which may or may not be in direct interaction with the Sec61p channel) [14, 15] producing FOS. This process of selective protein export from the ER to the cytosol followed by proteasomal degradation is termed ER associated degradation (ERAD). Cytosolic FOS produced are substrates for endo-ß-N-acetylglucosaminidase (ENGase) [16] and cytosolic α-mannosidase [17] ultimately forming a $Man_5GlcNAc_1$ species that is transported to the lysosome. However, glucosylated FOS are unable to gain entry to the lysosome for degradation [18] and their fate remains to be determined. In addition to $Man_5GlcNAc_1$ other small amounts of FOS including $Glc_1Man_5GlcNAc_1$, are produced by glycoproteins entering the ERAD pathway, and represent the normal default pathway for degradation [3].

Previously, we have shown that N–alkylated DNJ imino sugars inhibit ER glucosidases causing both an increase in the levels of cellular FOS and a change in the composition of the free oligosaccharide produced, i.e. an increase in the mono- and tri-glucosylated species was observed [3]. The

present study optimises the recovery of glucosylated FOS to allow full structural characterisation of 2-AA (anthranilic acid) fluorescently-labelled glycans using HPLC analysis, enzyme digestion and MALDI-TOF mass spectrometry. The FOS produced as a result of *N*B-DNJ treatment *in vivo*, have been measured in different tissues and the eventual fate of glucosylated FOS have been determined.

EXPERIMENTAL

Materials

Tissue culture media were from Gibco/Invitrogen, (Paisley, UK) or Sigma (Gillingham, UK). AnalaR and HPLC grade solvents were from VWR International. All other reagents were from Sigma. Water was Milli-Q™ grade. *N*B-DNJ was provided by Celltech (Slough, UK).

Cell Culture

HL60 cells were cultured in RPMI medium containing 10% foetal calf serum, 2 mM L-glutamine and 1% of a stock solution of 100 units/ml penicillin, 100 µg/ml streptomycin (Invitrogen).

*N*B-DNJ animal dosing

FVB/N or C57Bl/6 mice were maintained on a diet of powdered chow mixed with *N*B-DNJ at a range of dose levels up to 2400 mg/kg/day for 5 weeks as described previously [19]. Body fluids and tissues were harvested and stored at -20°C before extraction.

Clinical samples

Samples of plasma were obtained from an adult patient with Niemann-Pick disease type C (NP-C) treated with *N*B-DNJ (miglustat) for 16 months at variable doses but for the last 3 months before analysis, at 100 mg thrice daily, as described [20].

Urine samples were analysed from a juvenile Sandhoff disease patient treated with *N*B-DNJ for 6 months at a dose of 300 mg daily.

Free oligosaccharides (FOS) isolation

HL60 cells were cultured to high density (1×10^7 cells/ml) prior to growth in fresh medium containing *N*B-DNJ at varying concentrations. The cells were seeded at a lower density so as to achieve a high density at the end of the incubation period. Following cell culture the medium was removed and the cells were washed 3 times with PBS by centrifugation. Washed cells were stored at -20°C for a short time before thawing and dounce homogenisation in

water. An aliquot was taken for protein concentration determination using the Pierce BCA protein assay reagent, following manufacturers instructions. The maximum recovery of FOS was performed using the following conditions. The homogenate from 1-2 x 10^6 cells, (0.1-0.2 mg protein) was desalted and deproteinated by passage through a mixed-bed ion-exchange column {0.2 ml AG50W-X12 (H^+, 100-200 mesh) over 0.4 ml AG3-X4 (OH^-, 100-200 mesh)}, pre-equilibrated with water (5 × 1 ml). The homogenate was added to the column which was washed with 4 × 1 ml water, and the eluate collected. The extracted, purified FOS were then dried under vacuum or by freeze-drying.

Tissues (25mg wet weight) were frozen and thawed in 1 ml of water before homogenisation using a polytron. Murine serum and urine (100 µl), and human plasma (100 µl) and urine (1 ml) were used directly for FOS extraction as described above.

PGC chromatography

Glucose contained in the tissue extract from the mixed-bed ion-exchange column was removed prior to labelling using a 1 ml (25 mg) porous graphitized carbon (PGC) column (Thermo Electron, Runcorn, UK). The column was pre-equilibrated with 1 ml methanol, followed by 1 ml water, 1 ml acetonitrile containing 0.1% trifluoroacetic acid (TFA) and, finally, 2 x 0.5 ml water. After sample loading the column was washed with 2 x 0.5 ml water before oligosaccharides were eluted with 2 ml 50% acetonitrile containing 0.1% TFA.

Carbohydrate fluorescent labelling

The free oligosaccharides were labelled with anthranilic acid and purified using DPA-6S columns as described previously [21]. Free, uncongugated 2-AA was removed following phase splitting using ethyl acetate. 2-AA-Labelled sample (1 ml in water) was added to 1.5 ml of ethyl acetate and vortexed before separating into two phases by centrifugation at 3000 x *g* for 5 minutes. The upper phase was removed and a further 1.5 ml ethyl acetate was added and separation was repeated. Following a further addition of ethyl acetate the lower phase was removed and dried. The sample was then resuspended in

30 µl water before a preparative run by HPLC to allow isolation of individual peaks for further analysis.

Purification of fluorescently labelled FOS

Labelled oligosaccharides in 50 mM Tris/HCl buffer, pH 7.2 were purified using a Concanavalin A (ConA)–Sepharose 4B column (100µl packed resin). The column was pre-equilibrated with 2 × 1 ml water followed by 1 ml of 1 mM $MgCl_2$, 1 mM $CaCl_2$ and 1 mM $MnCl_2$ in water and finally 2 x 1 ml 50 mM Tris/HCl buffer, pH 7.2. The sample was added and allowed to pass through the column before washing with 2 x 1 ml 50 mM Tris/HCl buffer, pH 7.2. The ConA-bound, free oligosaccharides were then eluted with 2 x 1 ml hot (70°C) 0.5 M methyl α-D-mannopyranoside in 50 mM Tris/HCl buffer, pH 7.2.

Methyl α-D-mannopyranoside was removed from ConA-sepharose-purified 2-AA-labelled oligosaccharides in readiness for enzyme digestion using PGC chromatography as described above. No loss of FOS were observed following this procedure (data not shown).

Carbohydrate analysis by Normal-Phase high performance liquid chromatography (NP-HPLC)

ConA-Sepharose purified 2-AA-labeled oligosaccharides were separated by NP-HPLC (Waters, UK) using a 4.6 x 250 mm TSKgel Amide-80 column (Anachem, Luton, UK) with slight modifications to the published method [21]. Glucose units were determined, following comparison with a 2-AA-labeled glucose oligomer ladder (derived from a partial hydrolysate of dextran) external standard using Peak Time software (developed in-house).

The peak area of each 2-AA-labeled species was measured using Waters Empower software and converted to molar amounts using an experimentally-derived conversion factor (i.e., by 2-AA labelling a standard oligosaccharide of known concentration and measurement of peak area following HPLC separation).

Enzyme digests

Glycosidase digests were performed on the complete FOS populations and individually isolated peaks. Rat liver α-glucosidase I (0.1 M sodium phosphate buffer pH 7, containing 0.8% Lubrol-PX, 100 U/ml), and α-glucosidase II (80 mM Triethylamine buffer pH 7, containing 0.15 M NaCl and 10% glycerol, 5 mU/ml) were purified as described previously [22, 23]. *Aspergillus saitoi* α1,2-mannosidase (50 mM sodium acetate buffer pH 5, 0.46 mU/ml) and jack bean α-mannosidase (10 mM citric acid/sodium citrate buffer pH 4.5, containing 0.2 mM zinc acetate, 50 U/ml) were purified in-house. Following enzyme treatment for 16 h at 37°C, the reaction was stopped by addition of an equal volume of acetonitrile. The oligosaccharide reaction products were obtained after centrifugation through a 10,000 molecular weight cut off filter (pre-washed with 150 µl of water) at 7,000 x *g* for 45 minutes to remove protein before HPLC analysis.

***In vitro* glucosidase inhibition**

Free oligosaccharides were isolated from HL60 cells treated with 1 mM *N*B-DNJ, 2-AA-labelled and purified as substrates for either α-glucosidase I or II. Each fluorescence-labelled substrate was incubated with sufficient α-glucosidase I to generate 25% hydrolysis of $Glc_3Man_5GlcNAc_1$ or $Glc_3Man_9GlcNAc_2$ in a 30 min reaction time. Similarly, α-glucosidase II was incubated for 2 hours with $Glc_2Man_5GlcNAc_1$ and 20 minutes with $Glc_1Man_5GlcNAc_1$. In all cases linear degradation of substrate occurred over the time of incubation. Reactions were performed in the presence of varying concentrations of *N*B-DNJ, stopped by the addition of 30 µl acetonitrile and treated to remove protein as described above. Following HPLC separation of the reaction products the amount of digestion was quantified using peak area analysis.

Matrix Assisted Laser Desorption Ionising (MALDI) Mass Spectrometry of FOS

Positive-ion MALDI-TOF mass spectra were recorded with a Micromass TofSpec 2E reflectron-TOF mass spectrometer (Waters-Micromass (UK) Ltd.,

Manchester, UK) fitted with delayed extraction and a nitrogen laser (337 nm). The acceleration voltage was 20 kV; the pulse voltage was 3000 V; and the delay for the delayed extraction ion source was 500 ns. FOS, individually isolated by HPLC, were dried and resuspended in 100 µl of water. A 1 µl aliquot of each was mixed with 1 µl of a 50 mg/ml solution of 2,5-dihydroxybenzoic acid (2,5-DHB) in acetonitrile and allowed to air dry. The samples were re-crystallised from ethanol prior to analysis [24]. The *m/z* scale was calibrated using a 2-AA-labelled dextran hydrolysate ladder standard.

_N_B-DNJ extraction and purification from tissue or plasma samples

Plasma samples were centrifuged at 11,600 x *g* for 5 min and the supernatant was made up to 400 µl with water and 1.0 µg imino sugar internal standard (*N*-propyl-DNJ) added. Tissue samples were homogenized using an Ultra-Turrax T25 probe in 10% methanol in water (v/v) at concentrations of 130 mg (wet weight)/ml. After addition of an internal standard (as above) the homogenates were centrifuged at 100,000 x *g* for 15 min at 2°C. The supernatants were then used for imino sugar purification as described [25].

_N_B-DNJ quantitation following Cation-exchange chromatography

A Dionex BioLC with an ED50 electrochemical detector was used in all experiments. A CS10 analytical column (4 x 250 mm) was isocratically eluted with a solvent containing 50 mM sodium sulphate, 2.5 mM sulphuric acid and 5% (v/v) acetonitrile. The flow-rate was 1 ml/min and the column was maintained at a temperature of 40°C. A CMMS-II cation micro-membrane suppressor was used, with water as the regenerant, to convert the acidic eluant to basic conditions suitable for electrochemical detection. A triple-potential waveform was used for detection of carboxyanions. Imino sugar purified from plasma or tissue, was analysed as described in duplicate. The area under each peak, corresponding to the internal standard and *N*B-DNJ, was measured and after application of a predetermined response factor for the two imino sugars, the amount of *N*B-DNJ was calculated [25].

RESULTS

Characterisation of FOS produced in HL60 cells in the presence/absence of 1mM *N*B-DNJ

Previously we have analysed the effect of *N*B-DNJ on the generation of FOS in HL60 cells to gain insights into important cellular processes that participate in the glycoprotein-folding pathway [3]. A simplified FOS isolation protocol, with accurate extraction and purification efficiency determination, has been developed that negates the use of organic solvents and phase separation, as was previously employed [3]. This new method gave a greater than 90% recovery of total FOS as demonstrated by the recovery of known amounts of unlabelled oligosaccharides (see Supplemental Data). The use of hot (70°C) methyl-α-D-mannopyranoside was necessary to maximise recovery of oligosaccharides bound to Con A-Sepharose. The FOS species were analysed by HPLC following 2-AA fluorescent labelling and the structures characterised following a combination of enzyme digests (α-glucosidases I and II, *Aspergillus saitoi* α1,2-mannosidase and jack bean α-mannosidase), MALDI-TOF MS analysis and by comparison of glucose unit (GU) values to known oligosaccharide standards. The combined data from these experiments enabled us to compile a library of FOS structures in cells, including the percentage of each structure in terms of the total FOS population, following a 24 h period in the absence or presence of *N*B-DNJ, (Table 1).

Control FOS (Fig 1A and Table 1) showed a range of structures, with the major component (peak 4, 50.81%) being a $Man_5GlcNAc_1$ species with the structure, Manα2Manα2Manα3(Manα6)Manβ4GlcNAc. There was also, interestingly, a major component that was monoglucosylated $Man_5GlcNAc_1$ ($Glc_1Man_5GlcNAc_1$, peak 5, 16.09%) as well as further high-mannose structures similar to those found in previous studies [26, 27]. The addition of the α-glucosidase inhibitor, *N*B-DNJ, induced cells to produce a greater than three fold increase in total FOS, from 544 pmol/mg to 1470 pmol/mg. This increase was due to the production of mono-, di- and tri-glucosylated FOS species (Fig 1B and Table 1) with the major FOS being a tri-glucosylated

Man_5-based species, ($Glc_3Man_5GlcNAc_1$, peak 10A, 34%). These data are qualitatively similar to those reported previously using 2-aminobenzamide-labelling of large free oligosaccharides isolated from HL60 cells treated for 16 h with 1 mM *N*B-DNJ, but the improved method described here has increased recovery 2.5-3.0-fold [3]. In our previous study [3] a triglucosylated high-mannose oligosaccharide containing a single GlcNAc reducing terminus (predicted to be $Glc_3Man_5GlcNAc_1$) comprised 16.5% of the total population. The increase of this triglucosylated species using an increased time point (24 h) in the present study, is consistent with a greater effect on glucosidase I inhibition (see Fig 2A).

Kinetics of α-glucosidase inhibition

The data reported here support the idea that the measurement of FOS produced following imino sugar treatment may be used as a cellular based assay for α-glucosidase I and/or II inhibition. The build up of both the mono-glucosylated and the tri-glucosylated Man_5-based species were readily followed after 1 mM *N*B-DNJ treatment (Figure 2A). The initial step in the inhibition of N-linked oligosaccharide processing appears to be mediated by the reduction of α-glucosidase II activity as indicated by the rapid increase in the amount of $Glc_1Man_5GlcNAc_1$ observed (Figure 2A) before an equally rapid decline to control or below control levels. This increase, 153.5 ± 3.0 to 169.3 ± 5.0, was significant (95% confidence limits, Student's t-Test). A lag period before the effects of the inhibition of α-glucosidase I, resulting in the subsequent production of $Glc_3Man_5GlcNAc_1$, was observed supporting the preferential inhibition of α-glucosidase II seen in Figure 2A. This inhibition of glucosidase II in cultured cells was in direct contrast to the *in vitro* inhibition by *N*B-DNJ (Table 2). The inhibition of glucosidase II, in hydrolysing $Glc_1Man_5GlcNAc_1$, was appoximately 100-fold weaker than inhibition of glucosidase I using a triglucosylated substrate, irrespective of mannose structure or number of N-acetylglucosamine residues at the reducing terminus.

In cells, the amount of inhibition of α-glucosidase I activity in the presence of *N*B-DNJ, demonstrated by $Glc_3Man_5GlcNAc_1$ as a FOS marker, reached a plateau by 24 h, indicating that the maximum effective ER concentration of inhibitor had been achieved. Therefore, the concentration dependence of the α-glucosidase inhibition was investigated. Varying concentrations of *N*B-DNJ (0 - 1 mM *N*B-DNJ) were administered to HL60 cells for 24 h (Figure 2B). A concentration dependent increase in $Glc_3Man_5GlcNAc_1$ was observed with a near maximal level of tri-glucosylated FOS being reached at 1 mM.

Fate of FOS in cells

Previously published experiments examining FOS biosynthesis and degradation have been carried out over short time periods using metabolically-labelled substrate [12, 27]**.** The method developed here enables the study of cells that have undergone longer-term treatment with imino sugars. This method also allowed the study of the cellular fate of the FOS following removal of inhibition (Figure 3). *N*B-DNJ treatment for 72 h (Figure 3C) showed not only the build up of $Glc_3Man_5GlcNAc_1$, as seen after 24 h (Figure 3B), but also $Glc_3Man_4GlcNAc_1$. This indicated that $Glc_3Man_5GlcNAc_1$ was further degraded in the cell and that cytosolic α-mannosidase was, most probably, the enzyme responsible. However, the hydrolysis of $Glc_3Man_5GlcNAc_1$ to $Glc_3Man_4GlcNAc_1$ occurred at a much-reduced rate when compared to the hydrolysis of $Glc_3Man_{8\text{-}9}GlcNAc_1$ to $Glc_3Man_5GlcNAc_1$.

To investigate the origin of this $Glc_3Man_4GlcNAc_1$ species HL60 cells were treated for 24 h with 1 mM *N*B-DNJ to generate $Glc_3Man_5GlcNAc_1$ in the cytosol before removing the imino-sugar and hence, the α-glucosidase blockage. The cells were allowed to recover for 72 h before purification and analysis of the FOS (Figure 3D). The disappearance of the majority of the hyperglucosylated species was observed. However, a significant, though reduced, amount of the $Glc_3Man_4GlcNAc_1$ species was still present. These data indicate that the inhibition of ER-glucosidases was reversible but glucosylated FOS were retained in the cytosol before eventual clearance. The cytosolic α-mannosidase, or an as yet unidentified enzyme, is able to remove the accessible 4'Manα6 mannose residue to leave a linear $Glc_3Man_4GlcNAc_1$

species. The analysis of FOS 120 h post treatment revealed the continued presence of this tri-glucosylated FOS (results not shown). The eventual fate of glucosylated free oligosaccharides was therefore examined *in vivo*.

Effect of *N*B-DNJ on mouse tissue FOS production

FVB/N mice were treated with 1200 mg/kg/day of *N*B-DNJ for 5 weeks to maintain a steady state of *N*B-DNJ in their serum. An overnight urine collection after 5 weeks treatment was performed using a metabolic cage. Heart, kidney, lung, liver, brain and spleen (25 mg wet weight tissue) were used for FOS analysis. These were compared to the same samples obtained from age-matched untreated FVB/N mice. The effect of *N*B-DNJ on total FOS production was pronounced in all samples, with a significant increase (at the 95% confidence level) in FOS amounts (Table 3, and supplemental data) and the appearance of glucosylated high-mannose FOS in the samples (Figure 4 and Table 1). In heart (Fig 4A), $Glc_3Man_4GlcNAc_1$ was present in the largest amount (peak 6A, 37%) with the appearance of a lesser amount of $Glc_1Man_4GlcNAc_1$ (peak 2A, 17.1%). The oligosaccharide $Glc_1Man_4GlcNAc_1$ was the major glycan observed in kidney (48.3%, Fig 4B), lung (30.4%, Fig 4C) and liver (15.3%, Fig 4D). The FOS profiles for kidney and lung were very similar with respect to the presence of new minor species (peaks 1B, 5 and 10C, Fig 4B & C**)** following treatment with *N*B-DNJ. In liver these same peaks appeared but peak 10C was present as a larger amount of the total FOS (9.7%) when compared with all other tissues. This new species 10C, not seen in *N*B-DNJ treated HL60 cells, was found to be a $GlcNAc_2$-containing FOS, as demonstrated by MALDI-TOF mass spectrometry analysis (results not shown), with the structure $Glc_1Man_7GlcNAc_2$. The origin of this chitobiose-containing species is being explored further. In brain, the appearance of a small but significant amount of $Glc_1Man_5GlcNAc_1$ (peak 5, 6.3%, Fig 4E) was seen, with a small increase in $Glc_1Man_4GlcNAc_1$ also observed. However, in brain, the non-glucosylated species were still the majority of FOS observed. The liver had the largest amount of FOS observed prior to and following *N*B-DNJ treatment (29.4 and 86.2 pmol/mg, respectively). The heart differed from the other tissues examined, as $Glc_3Man_4GlcNAc_1$ was the major glycan

observed following treatment. This is probably due to a greater inhibition of α-glucosidase I rather than α-glucosidase II in this tissue. The occurrence of greater α-glucosidase I inhibition was also seen in the hind muscle and red blood cells of mice treated with *N*B-DNJ (data not shown). In spleen greater inhibition of α-glucosidase II was again observed consistent with the production of a $Glc_1Man_4GlcNAc_1$ species.

Murine serum and urine were analysed for FOS (Figure 5 and Table 3), and sera were also used to determine *N*B-DNJ concentration. An average value of 26.4 μM *N*B-DNJ was found in treated mice. The FOS analysis closely matched the situation observed in tissues, with $Glc_1Man_4GlcNAc_1$ (peak 2A, Fig 5 and Table 2) being the major glucosylated FOS produced following *N*B-DNJ treatment. Again, there was a statistically significant (95% confidence level, Student's t-Test) increase in the total amount of FOS measured with an approximate a two-fold and three-fold increase in serum and urine, respectively. The $Glc_1Man_4GlcNAc_1$ species, therefore, may represent the end-clearance product of glucosylated FOS from murine tissues. This analysis also demonstrated that the clearance of higher glucosylated FOS from tissues to urine, via serum, was also possible as $Glc_{1/3}Man_5GlcNAc_1$ and $Glc_1Man_7GlcNAc_2$ FOS, observed in both tissues and serum, were also found in urine.

_N_B-DNJ production of glucosylated FOS in murine serum is time and dose dependent

Serum was obtained from mice (n=3) treated with 2400 mg/kg/day of *N*B-DNJ for 2, 5, 9, 13 and 17 days. The serum was pooled and an aliquot was used for FOS analysis (Figure 6A). The level of $Glc_1Man_4GlcNAc_1$ produced in serum, as a result of *N*B-DNJ treatment, reached a plateau after 5 days. A similar affect was seen on $Glc_1Man_4GlcNAc_1$ levels in the serum of mice treated with escalating doses of *N*B-DNJ for five weeks with a maximal level achieved at the highest dose, 2400 mg/kg/day (Figure 6B). This matches those data in cultured cells where there was a time- and concentration-dependent production of glucosylated FOS.

Reversal of α-glucosidase inhibition

Mice (C57Bl/6) were treated with 1200 mg/kg/day *N*B-DNJ for 5 weeks prior to removal from the drug-treated diet and placed in a metabolic cage for 0.5, 1, 2, 4, 6 and 8 h before sacrificing. The sera and urine of these animals were then used for FOS analysis, and *N*B-DNJ concentration determination in the serum (Figure 6C). The amount of *N*B-DNJ declined rapidly in the serum following drug removal and was undetectable after 4 h, with an estimated half life of 1.34 h**.** The FOS produced as a result of *N*B-DNJ induced glucosidase inhibition had a similar serum half-life of 1.86 h and were finally cleared transrenally to urine with a half-life of 3.72 h. It was noticed that following *N*B-DNJ treatment the thymus was significantly reduced in size, as previously reported by this laboratory [19]. Thymi of mice sacrificed following a 4 h removal from *N*B-DNJ were similar in appearance to control mice, suggesting that the effect on thymus acellularity is a direct effect of the drug. Following the clearance of *N*B-DNJ from serum there was a lag period of approximately 4 h until glucosylated FOS returned to control levels in serum and 12 h in urine.

FOS in human samples following *N*B-DNJ treatment

To demonstrate that this technique was applicable to human samples, plasma and urine were obtained from human patients with lysosomal storage disorders that were undertaking SRT with *N*B-DNJ. Pre- and post-treatment samples were analysed for *N*B-DNJ and FOS in the plasma, and FOS in the urine (Figure 7). The plasma was from a patient suffering from Niemann-Pick type C (NP-C) treated with 100-300 mg/day *N*B-DNJ [20]. Treatment for 16 months at this variable dose gave a plasma concentration that averaged 2 ± 0.8 μM [20], considerably lower than concentrations used to inhibit glucosidases in cultured cells. The urine was from a juvenile Sandhoff patient administered with 300 mg/day *N*B-DNJ for 6 months. The analysis of FOS species in plasma and urine revealed an increase in the monoglucosylated glycans $Glc_1Man_4GlcNAc_1$ and $Glc_1Man_5GlcNAc_1$, and the tri-glucosylated species $Glc_3Man_4GlcNAc_1$ (Figure 7), indicating that glucosidase inhibition had been achieved following treatment.

DISCUSSION

The aims of this study were to understand and characterise alterations in the biochemical pathways induced by imino sugar glucosidase inhibitors. Therefore, we have developed protocols that accurately measure FOS produced in cells as a functional consequence of ER-glucosidase inhibition. In the absence or presence of α-glucosidase inhibitors, misfolded glycoproteins are translocated to the cytosol where PNGase releases oligosaccharides and the protein is degraded by the proteosome. The free oligosaccharides are substrates for cytosolic ENGase that generates FOS containing a single reducing-terminal GlcNAc [28], and subsequently cytosolic α-mannosidase, which preferentially recognises these FOS that are trimmed to a $Man_5GlcNAc_1$ structure [29-31]. This structure, Manα2Manα2Manα3(Manα6)Manβ4GlcNAc, is similar to the $Man_5GlcNAc_2$ structure observed attached to dolichol on the extracellular leaflet of the ER. An ATP-dependent process subsequently translocates the non-glucosylated $Man_5GlcNAc_1$ into the lysosome for degradation [30]. With a functional FOS catabolic pathway in cells it is no surprise that $Man_5GlcNAc_1$ is the major species in control cells. This species may represent the normal flux of misfolded protein secreted via the calnexin/calreticulin-mediated ERAD pathway and is either resident in the cytoplasm or the lysosome.

The major species observed following *N*B-DNJ treatment in HL60 cells was a $Glc_3Man_5GlcNAc_1$ oligosaccharide derived subsequent to retrotranslocation of misfolded and hyperglucosylated proteins from the ER to the cytosol. This oligosaccharide may be unable to translocate into the lysosome for degradation since there is some evidence for the lack of an efficient glucosylated FOS lysosomal transporter [18,32]. Therefore, an increase in FOS is observed in agreement with previous studies [3].

When high concentrations of *N*B-DNJ (1 mM) were used to treat cells, α-glucosidase inhibition reached a plateau, indicative of a time-dependent *N*B-DNJ equilibration rate (cytosol-ER). The initial build up of mono-glucosylated FOS at short time periods (0-2 h) before triglucosylated FOS are generated reveals the potent cellular inhibition of α-glucosidase II, compared to α-glucosidase I, and contrasts markedly with the inhibition of these enzymes

using *in vitro* assays, where, on the basis of IC_{50} values, *N*B-DNJ is 100 times more efficient at inhibiting α-glucosidase I than II. The very small amount of diglucosylated FOS produced demonstrates that *N*B-DNJ is relatively poor at preventing the removal of the first α1,2-linked glucose. This reflects the kinetics of glucosidase I and II action in the ER, resulting in the efficient and rapid hydrolysis of tri- and di-glucosylated glycans to mono-glucosylated glycans to allow interaction with calnexin/calreticulin chaperones. The concentration-dependence of *N*B-DNJ inhibition suggests that a maximum level of DNJ-based imino sugar is achieved in the ER beyond which some physiological aspect of the ER prevents further import or activates ER-exit of imino sugar.

The longer half-life of mono-glucosylated glycans, when compared to tri-and di-glucosylated species, is due to the slower hydrolysis rate of the proximal glucose residue by glucosidase II [33-35]. This contributes to a more favourable environment for *N*B-DNJ inhibition of this step. Removal of the first glucose residue by glucosidase I and the second glucose residue by glucosidase II in cultured cells probably occurs at close to their limiting rates (V_{max}), where addition of a competitive inhibitor has a limited effect on the observed rate. Removal of the third glucose residue by glucosidase II is much slower, suggesting that the rate is not close to V_{max} and under these conditions a competitive inhibitor has a much greater effect on the rate. Since glucosidase II and calnexin both compete for the same substrate in the ER, $Glc_1Man_9GlcNAc_2$-protein, if glucosidase II is unable to hydrolyse substrate bound to calnexin, the presence of calnexin will significantly reduce the free substrate concentration, hence reducing the rate. Alternatively, if glucosidase II is able to hydrolyse substrate bound to calnexin, the presence of calnexin is likely to change K_m. An increase in K_m would also result in a reduced rate. Both possibilities have the same functional outcome; the rate of removal of the proximal glucose residue is reduced in cells and hence is more sensitive to the presence of a competitive inhibitor, resulting in a greater accumulation of mono-glucosylated glycans.

How do cells then deal with glucosylated FOS? Following treatment with *N*B-DNJ (24 and 72 h) the major proportion of FOS observed are $Glc_{1-3}Man_{4-5}GlcNAc_1$ structures. The presence of $Glc_{1-3}Man_4GlcNAc_1$ FOS demonstrates that cytosolic α-mannosidase, or an unknown α-mannosidase, may act on $Man_5GlcNAc_1$-containing FOS. The lack of lysosomal degradation, and increased cellular residence time of glucosylated $Man_5GlcNAc_1$-containing FOS observed, may explain the higher concentration of glucosylated $Man_4GlcNAc_1$-containing FOS observed following the 72 h treatment with *N*B-DNJ. Long-term (72 h) treatment with *N*B-DNJ, where a significant quantity of $Glc_3Man_4GlcNAc_1$ is generated, followed by removal of inhibitor, reveals a slow decline in the amount of cellular $Glc_3Man_4GlcNAc_1$. Analysis of the extracellular medium shows that $Glc_3Man_4GlcNAc_1$ is present (results not shown) and suggests that some mechanism exists for cellular export of glucosylated FOS. The recovery experiments demonstrate that mono-glucosylated FOS, which naturally occur, and also the tri-glucosylated FOS produced in the presence of a glucosidase inhibitor are removed from the cell. In Lec23 cells (glucosidase I deficient cells), $Glc_3Man_5GlcNAc_1$ is eventually cleared by an unknown mechanism at cell confluence [32].

The $Man_4GlcNAc_1$ species observed in control cells is presumably not formed in the lysosome following the action of lysosomal α-6-mannosidase as this enzyme preferentially removes the α6Man residue from a Manα6Manβ4GlcNAcβ1 structure [36]. Although the cellular location of this species has yet to be determined it is probable that this is produced as a result of a cytosolic α-mannosidase activity.

The methods developed here in tissue culture cells have been extended to characterise the pathway for FOS export from tissues *in vivo* to reveal cellular clearance and catabolic end-products. When administered to mouse, *N*B-DNJ causes an increase in glucosylated FOS in tissues, sera and urine, similar to the effect previously demonstrated in cultured cells. The tissues with normally high concentrations of FOS prior to *N*B-DNJ treatment, provided the greatest increase in glucosylated FOS, presumably due to greater glycoprotein synthesis/turnover rates in the cells of these tissues that would contribute to the pool of ERAD substrates. The major species produced were

$Glc_1Man_4GlcNAc_1$ and $Glc_3Man_4GlcNAc_1$ species, which demonstrates quite clearly than once glucosylated FOS are produced in the cytosol, the cellular catabolic endpoint is a glucosylated $Man_4GlcNAc_1$ structure, not a glucosylated $Man_5GlcNAc_1$ structure as previously thought [32]. The analysis of the tissue FOS supports the low dose data in cultured cells, with a monoglucosylated species being the major species produced following treatment in most tissues. At steady-state concentrations of *N*B-DNJ there was sufficient access to the ER of cells to selectively inhibit α-glucosidase II-mediated hydrolysis of the Glcα3Man linkage. As observed in cultured cells this is the more inhibitor-sensitive step in the glycosylation pathway. However, the heart appears to show preferential α-glucosidase I inhibition as $Glc_3Man_4GlcNAc_1$ was the major species produced. This is not a result of increased *N*B-DNJ retention in the heart [37] but could result from a low level of N-linked glycoprotein biosynthesis in the heart.

The time-dependence of *N*B-DNJ administration on FOS production shows that a steady-state of α-glucosidase II inhibition, as evidenced by the detection of $Glc_1Man_4GlcNAc_1$, is reached after 5 days. A similar effect of α-glucosidase inhibition was seen with 1200 mg/kg/day and 2400 mg/kg/day doses, indicating that sufficient concentration of *N*B-DNJ had been reached to inhibit preferentially α-glucosidase II. Previous examination of the effect of 2400mg/kg/day of *N*B-DNJ for 14 days treatment on C57Bl/6 mice [19] examined changes to mature glycoproteins on a specific cell type (splenocytes), whereas the FOS assay developed here is more sensitive in revealing the effects of α-glucosidase inhibition on all tissue-resident cells. The relatively short serum half-life of *N*B-DNJ in mouse is approximately four times less than the half-life in man [7], in keeping with the higher metabolic rate per kilogram mass seen in mouse compared to man [38].

The present study has demonstrated that analysis of FOS in ER-α-glucosidase inhibitor-treated higher vertebrates reveals accurate and measurable biomarkers of the effects of *N*B-DNJ administration. The protocols developed here have shown that the FOS generation in tissue-cultured cells closely parallels that seen in both mouse and man. These protocols can be used non-invasively to analyse the effects on ER-

glucosidase inhibition on protein folding by monitoring for the presence of glucosylated FOS in urine.

ACKNOWLEDGEMENTS

The authors thank Naomi Wright at the Dept of Medicine, Cambridge for patient sample collection and the Glycobiology Institute and BBSRC (DSA) for support.

REFERENCES

1 Dwek, R. A., Butters, T. D., Platt, F. M. and Zitzmann, N. (2002) Targeting glycosylation as a therapeutic approach. Nat. Rev. Drug Discov. **1**, 65-75

2 Mellor, H. R., Neville, D. C., Harvey, D. J., Platt, F. M., Dwek, R. A. and Butters, T. D. (2004) Cellular effects of deoxynojirimycin analogues: uptake, retention and inhibition of glycosphingolipid biosynthesis. Biochem. J. **381**, 861-866

3 Mellor, H. R., Neville, D. C., Harvey, D. J., Platt, F. M., Dwek, R. A. and Butters, T. D. (2004) Cellular effects of deoxynojirimycin analogues: inhibition of N-linked oligosaccharide processing and generation of free glucosylated oligosaccharides. Biochem. J. **381**, 867-875

4 Mellor, H. R., Nolan, J., Pickering, L., Wormald, M. R., Platt, F. M., Dwek, R. A., Fleet, G. W. and Butters, T. D. (2002) Preparation, biochemical characterization and biological properties of radiolabelled N-alkylated deoxynojirimycins. Biochem. J. **366**, 225-233

5 Butters, T. D., Dwek, R. A. and Platt, F. M. (2000) Inhibition of glycosphingolipid biosynthesis: application to lysosomal storage disorders. Chem. Rev. **100**, 4683-4696

6 Platt, F. M., Neises, G. R., Dwek, R. A. and Butters, T. D. (1994) N-butyldeoxynojirimycin is a novel inhibitor of glycolipid biosynthesis. J. Biol. Chem. **269**, 8362-8365

7 Cox, T., Lachmann, R., Hollak, C., Aerts, J., van Weely, S., Hrebicek, M., Platt, F., Butters, T., Dwek, R., Moyses, C., Gow, I., Elstein, D. and Zimran, A. (2000) Novel oral treatment of Gaucher's disease with N-butyldeoxynojirimycin (OGT 918) to decrease substrate biosynthesis. Lancet **355**, 1481-1485

8 Block, T. M., Lu, X., Mehta, A. S., Blumberg, B. S., Tennant, B., Ebling, M., Korba, B., Lansky, D. M., Jacob, G. S. and Dwek, R. A. (1998) Treatment of chronic hepadnavirus infection in a woodchuck animal model with an inhibitor of protein folding and trafficking. Nat. Med. **4**, 610-614

9 Zitzmann, N., Mehta, A. S., Carrouee, S., Butters, T. D., Platt, F. M., McCauley, J., Blumberg, B. S., Dwek, R. A. and Block, T. M. (1999) Imino sugars inhibit the formation and secretion of bovine viral diarrhea virus, a pestivirus model of hepatitis C virus: implications for the development of broad spectrum anti-hepatitis virus agents. Proc. Natl. Acad. Sci. U S A **96**, 11878-11882

10 van den Broek, L. A. G. M., Vermaas, D. J., van Kemenade, F. J., Tan, M. C. C. A., Rotteveel, F. T. M., Zandberg, P., Butters, T., Miedema, F., Ploegh, H. L. and van Boeckel, C. A. A. (1994) Synthesis of oxygen-substituted N-alkyl 1-deoxynojirimycin derivatives; aza sugar α-glucosidase inhibitors showing antiviral (HIV-1) and immunosuppresive activity. Recueil des Travaux Chimiques des Pays-Bas **113**, 507-516

11 Spiro, M. J. and Spiro, R. G. (1991) Potential regulation of N-glycosylation precursor through oligosaccharide-lipid hydrolase action and glucosyltransferase-glucosidase shuttle. J. Biol. Chem. **266**, 5311-5317

12 Spiro, M. J. and Spiro, R. G. (2001) Release of polymannose oligosaccharides from vesicular stomatitis virus G protein during endoplasmic reticulum-associated degradation. Glycobiology **11**, 803-811

13 Wiertz, E. J., Tortorella, D., Bogyo, M., Yu, J., Mothes, W., Jones, T. R., Rapoport, T. A. and Ploegh, H. L. (1996) Sec61-mediated transfer of a membrane protein from the endoplasmic reticulum to the proteasome for destruction. Nature **384**, 432-438

14 Li, G., Zhou, X., Zhao, G., Schindelin, H. and Lennarz, W. J. (2005) Multiple modes of interaction of the deglycosylation enzyme, mouse peptide N-glycanase, with the proteasome. Proc. Natl. Acad. Sci. U S A **102**, 15809-15814

15 Spiro, R. G. (2004) Role of N-linked polymannose oligosaccharides in targeting glycoproteins for endoplasmic reticulum-associated degradation. Cell Mol. Life Sci **61**, 1025-1041

16 Suzuki, T., Yano, K., Sugimoto, S., Kitajima, K., Lennarz, W. J., Inoue, S., Inoue, Y. and Emori, Y. (2002) Endo-beta-N-acetylglucosaminidase, an enzyme involved in processing of free oligosaccharides in the cytosol. Proc. Natl. Acad. Sci. U S A **99**, 9691-9696

17 Shoup, V. A. and Touster, O. (1976) Purification and characterization of the alpha-D-mannosidase of rat liver cytosol. J. Biol. Chem. **251**, 3845-3852

18 Saint-Pol, A., Codogno, P. and Moore, S. E. (1999) Cytosol-to-lysosome transport of free polymannose-type oligosaccharides. Kinetic and specificity studies using rat liver lysosomes. J. Biol. Chem. **274**, 13547-13555

19 Platt, F. M., Reinkensmeier, G., Dwek, R. A. and Butters, T. D. (1997) Extensive glycosphingolipid depletion in the liver and lymphoid organs of mice treated with N-butyldeoxynojirimycin. J. Biol. Chem. **272**, 19365-19372

20 Lachmann, R. H., te Vruchte, D., Lloyd-Evans, E., Reinkensmeier, G., Sillence, D. J., Fernandez-Guillen, L., Dwek, R. A., Butters, T. D., Cox, T. M. and Platt, F. M. (2004) Treatment with miglustat reverses the lipid-trafficking defect in Niemann-Pick disease type C. Neurobiol. Dis. **16**, 654-658

21 Neville, D. C., Coquard, V., Priestman, D. A., Te Vruchte, D. J., Sillence, D. J., Dwek, R. A., Platt, F. M. and Butters, T. D. (2004) Analysis of fluorescently labeled glycosphingolipid-derived oligosaccharides following ceramide glycanase digestion and anthranilic acid labeling. Anal. Biochem. **331**, 275-282

22 Karlsson, G. B., Butters, T. D., Dwek, R. A. and Platt, F. M. (1993) Effects of the imino sugar N-butyldeoxynojirimycin on the N-glycosylation of recombinant gp120. J. Biol. Chem. **268**, 570-576

23 Olafson, R. W., Thomas, J. R., Ferguson, M. A., Dwek, R. A., Chaudhuri, M., Chang, K. P. and Rademacher, T. W. (1990) Structures of the N-linked oligosaccharides of Gp63, the major surface glycoprotein, from Leishmania mexicana amazonensis. J. Biol. Chem. **265**, 12240-12247

24 Harvey, D. J. (1993) Quantitative aspects of the matrix-assisted laser desorption mass spectrometry of complex oligosaccharides. Rapid Commun. Mass Spectrom. **7**, 614-619

25 Mellor, H. R., Adam, A., Platt, F. M., Dwek, R. A. and Butters, T. D. (2000) High-performance cation-exchange chromatography and pulsed amperometric detection for the separation, detection, and quantitation of N-alkylated imino sugars in biological samples. Anal .Biochem. **284**, 136-142

26 Cacan, R., Duvet, S., Labiau, O., Verbert, A. and Krag, S. S. (2001) Monoglucosylated oligomannosides are released during the degradation process of newly synthesized glycoproteins. J. Biol. Chem. **276**, 22307-22312

27 Moore, S. E. and Spiro, R. G. (1994) Intracellular compartmentalization and degradation of free polymannose oligosaccharides released during glycoprotein biosynthesis. J. Biol. Chem. **269**, 12715-12721

28 Moore, S. E., Bauvy, C. and Codogno, P. (1995) Endoplasmic reticulum-to-cytosol transport of free polymannose oligosaccharides in permeabilized HepG2 cells. EMBO J. **14**, 6034-6042

29 Haeuw, J. F., Strecker, G., Wieruszeski, J. M., Montreuil, J. and Michalski, J. C. (1991) Substrate specificity of rat liver cytosolic alpha-D-mannosidase. Novel degradative pathway for oligomannosidic type glycans. Eur. J. Biochem. **202**, 1257-1268

30 Tulsiani, D. R. and Touster, O. (1987) Substrate specificities of rat kidney lysosomal and cytosolic alpha-D-mannosidases and effects of

swainsonine suggest a role of the cytosolic enzyme in glycoprotein catabolism. J. Biol. Chem. **262**, 6506-6514

31 Yamagishi, M., Ishimizu, T., Natsuka, S. and Hase, S. (2002) Co(II)-regulated substrate specificity of cytosolic alpha-mannosidase. J. Biochem. (Tokyo) **132**, 253-256

32 Durrant, C. and Moore, S. E. (2002) Perturbation of free oligosaccharide trafficking in endoplasmic reticulum glucosidase I-deficient and castanospermine-treated cells. Biochem. J. **365**, 239-247

33 Cumpstey, I., Butters, T. D., Tennant-Eyles, R. J., Fairbanks, A. J., France, R. R. and Wormald, M. R. (2003) Synthesis of fluorescence-labelled disaccharide substrates of glucosidase II. Carbohydr. Res. **338**, 1937-1949

34 Kaushal, G. P., Pan, Y. T., Tropea, J. E., Mitchell, M., Liu, P. and Elbein, A. D. (1988) Selective inhibition of glycoprotein-processing enzymes. Differential inhibition of glucosidases I and II in cell culture. J. Biol. Chem. **263**, 17278-17283

35 Petrescu, A. J., Butters, T. D., Reinkensmeier, G., Petrescu, S., Platt, F. M., Dwek, R. A. and Wormald, M. R. (1997) The solution NMR structure of glucosylated N-glycans involved in the early stages of glycoprotein biosynthesis and folding. EMBO J. **16**, 4302-4310

36 Daniel, P. F., Winchester, B. and Warren, C. D. (1994) Mammalian alpha-mannosidases--multiple forms but a common purpose? Glycobiology **4**, 551-566

37 Andersson, U., Butters, T. D., Dwek, R. A. and Platt, F. M. (2000) N-butyldeoxygalactonojirimycin: a more selective inhibitor of

glycosphingolipid biosynthesis than N-butyldeoxynojirimycin, in vitro and in vivo. Biochem. Pharmacol. **59**, 821-829

38 Spatz, H. C. (1991) Circulation, metabolic rate, and body size in mammals. J. Comp. Physiol. [B] **161**, 231-236

FIGURE LEGENDS

Figure 1. HPLC analysis of 2-AA fluorescently labelled free oligosaccharides (FOS).

HL60 cells were homogenised and FOS extracted as described in the text. Following 2-AA labelling FOS were separated by HPLC. (A) control cells and (B) cells treated with 1 mM *N*B-DNJ for 24 h. Peaks are numbered and structurally annotated as shown in Table 1.

Figure 2: Glucosylated FOS in HL60 cells treated with *N*B-DNJ.

(A) Production of monoglucosylated FOS (■, $Glc_1Man_5GlcNAc_1$) and triglucosylated FOS (▲,$Glc_3Man_5GlcNAc_1$) in the presence of 1 mM *N*B-DNJ for 24 h. (B) Production of triglucosylated FOS (■,$Glc_3Man_5GlcNAc_1$) after 24 h of treatment with varying concentrations (0-1 mM). The mean values, in pmol/mg protein, of oligosaccharides obtained from triplicate experiments (± SD) are shown, using equivalent cell numbers in each experiment. Independent experiments showed that cell number was proportional to protein concentration, as determined by the BCA assay.

Figure 3: Long-term treatment of cells with *N*B-DNJ and recovery.

2-AA fluorescently-labelled FOS were extracted from (A) HL60 control cells (B) HL60 cells treated with 1 mM *N*B-DNJ for 24 h (C) HL60 cells treated with 1 mM *N*B-DNJ for 72 h and (D) HL60 cells treated with 1 mM *N*B-DNJ for 24 h followed by a 72 h period after inhibitor removal. The HPLC profiles are

representative examples of several experiments and are drawn to the same scale of fluorescence intensity.

Figure 4. HPLC analysis of 2-AA fluorescently-labelled FOS from murine tissues.

Tissue from FVB/N control mice (black) and mice treated with 1200mg/kg/day (red) were homogenised and FOS extracted as described in the text. Following 2-AA labelling FOS were separated following NP-HPLC. (A) Heart, (B) Kidney, (C) Lung, (D) Liver, (E) Brain and (F) Spleen. Peaks are numbered and structures delineated as shown in Table 1.

Figure 5. HPLC analysis of 2-AA fluorescently labelled free oligosaccharides (FOS) from murine serum and urine.

Serum and urine from FVB/N control mice (black) and mice treated with 1200mg/kg/day *N*B-DNJ (red). FOS were extracted as described in the text. Following 2-AA labelling FOS were separated following NP-HPLC. (A) Serum and (B) Urine. Peaks are numbered and structures delineated as shown in Table 1.

Figure 6. Glucosylated FOS in serum of mice treated with *N*B-DNJ is time and dose dependent, and reversible.

(A) Monoglucosylated FOS ($Glc_1Man_4GlcNAc_1$) in pooled serum (nmol/ml) of C57Bl/6 mice following treatment with 2400mg/kg/day *N*B-DNJ for 0-17 days. (B) Monoglucosylated FOS ($Glc_1Man_4GlcNAc_1$) in serum (nmol/ml) of C57Bl/6 mice following treatment with 0-2400mg/kg/day *N*B-DNJ for 5 weeks. (C) Monoglucosylated FOS ($Glc_1Man_4GlcNAc_1$) in serum (■) and pooled urine (▼) expressed as nmol/ml, in C57Bl/6 mice following treatment with 1200 mg/kg/day *N*B-DNJ for 5 weeks and subsequent removal for 0.5 - 16 h. *N*B-DNJ concentration in serum (µg/ml) over the same time period is shown (▲). Where appropriate, the mean value for five animals per treatment group is shown, ± SD.

Figure 7. HPLC analysis of 2-AA fluorescently-labelled FOS from human serum and urine

FOS were extracted from human serum and urine, pre-treatment (dark line) and post-treatment (light line) with *N*B-DNJ as described in the text. Following 2-AA labelling FOS were separated by NP-HPLC. (A) Serum from a NP-C patient treated with 100-300 mg/day for 16 months and (B) Urine from a juvenile Sandhoff patient treated with 300 mg/day for 6 months. FOS are numbered as in Figure 1 and structures delineated as shown in Table 1.

Figure 1

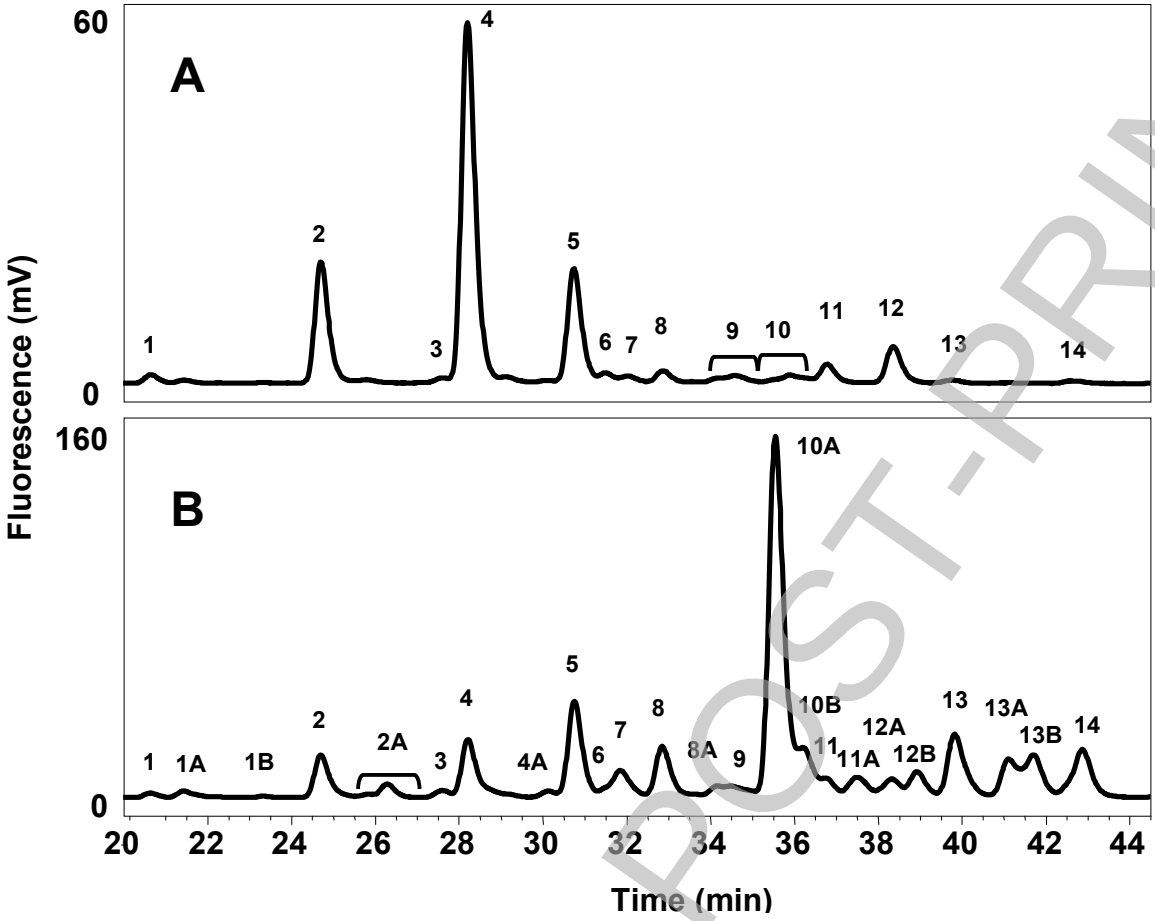

Figure 2

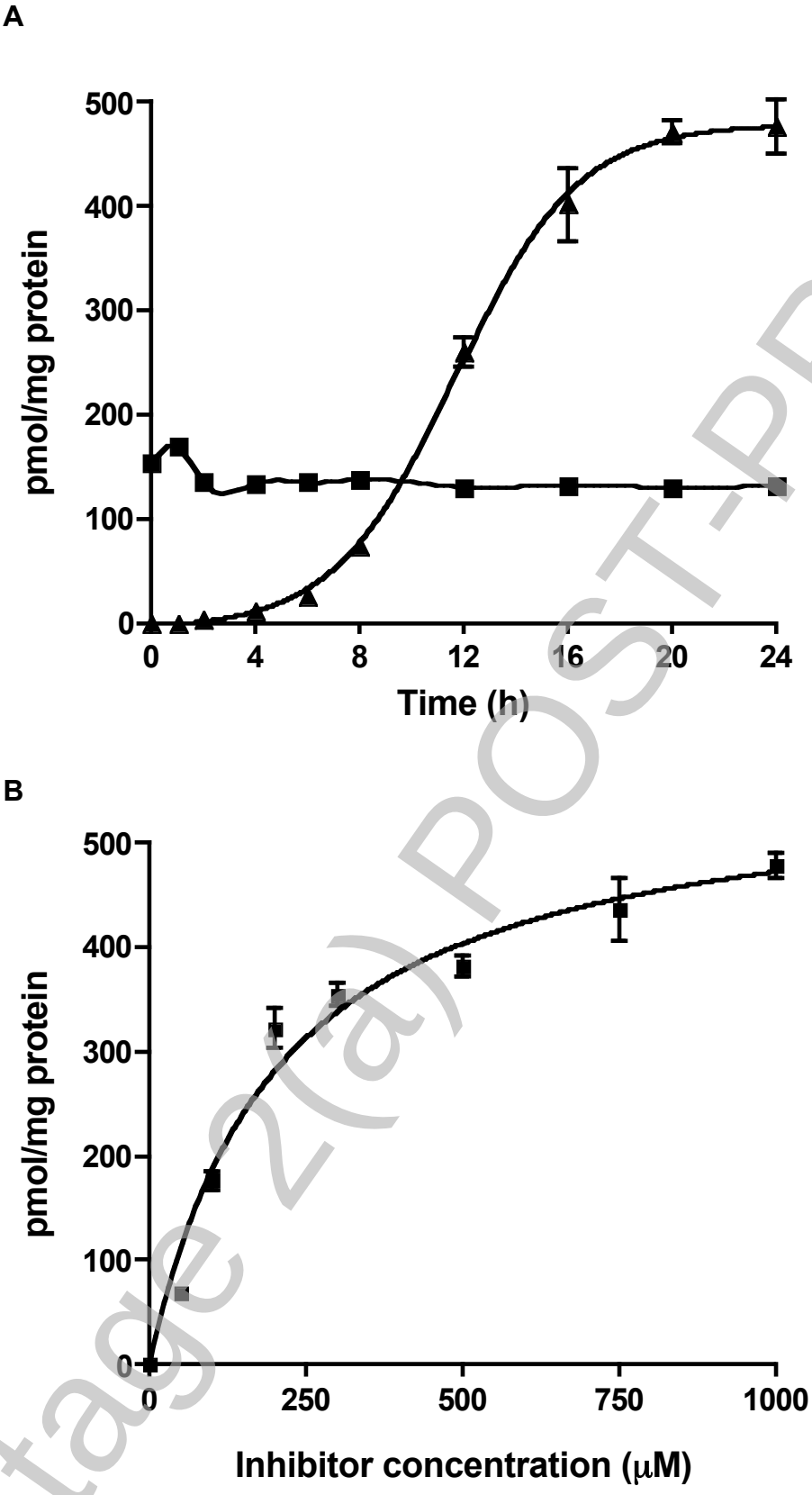

Figure 3

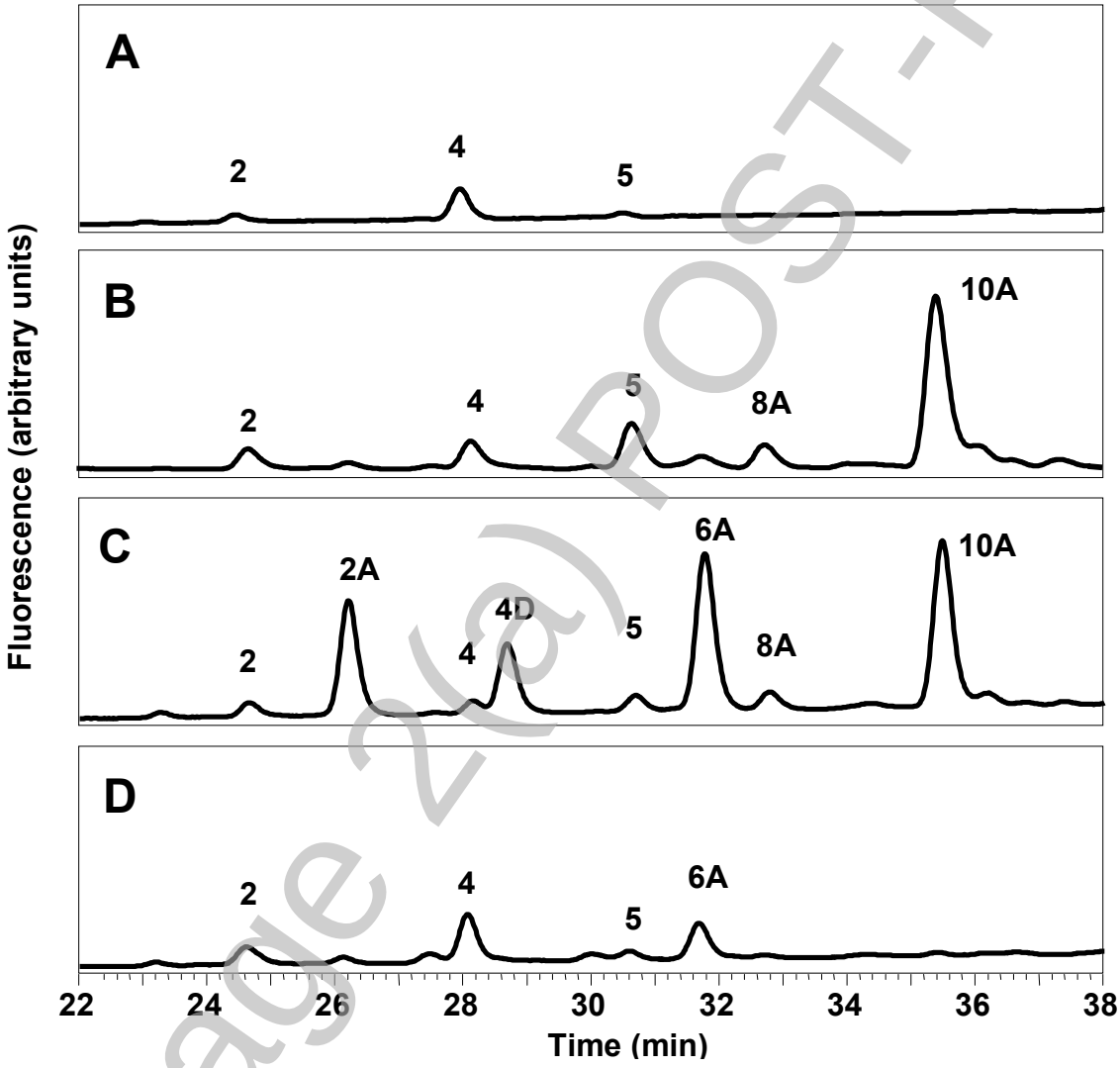

Figure 4

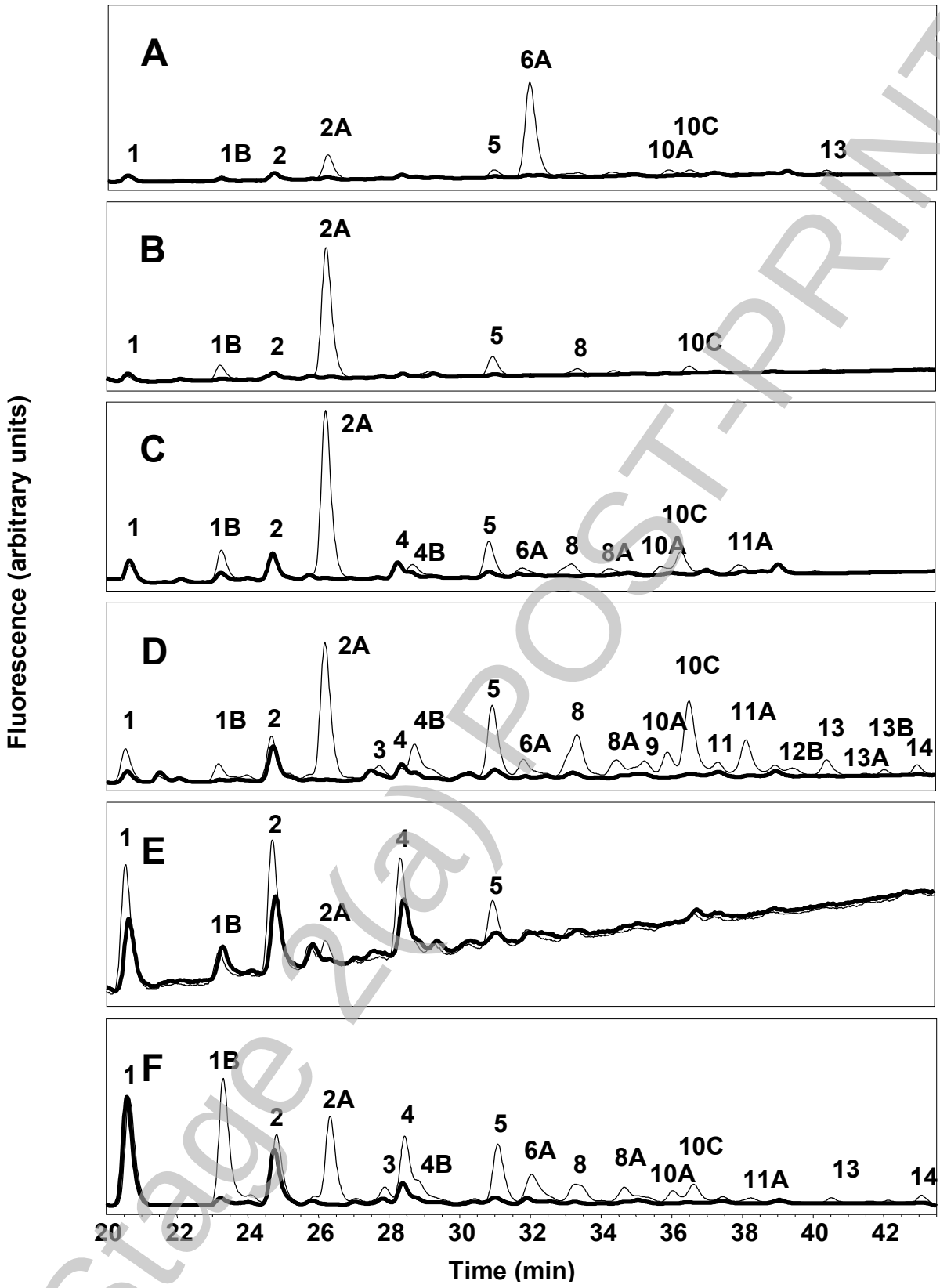

Figure 5

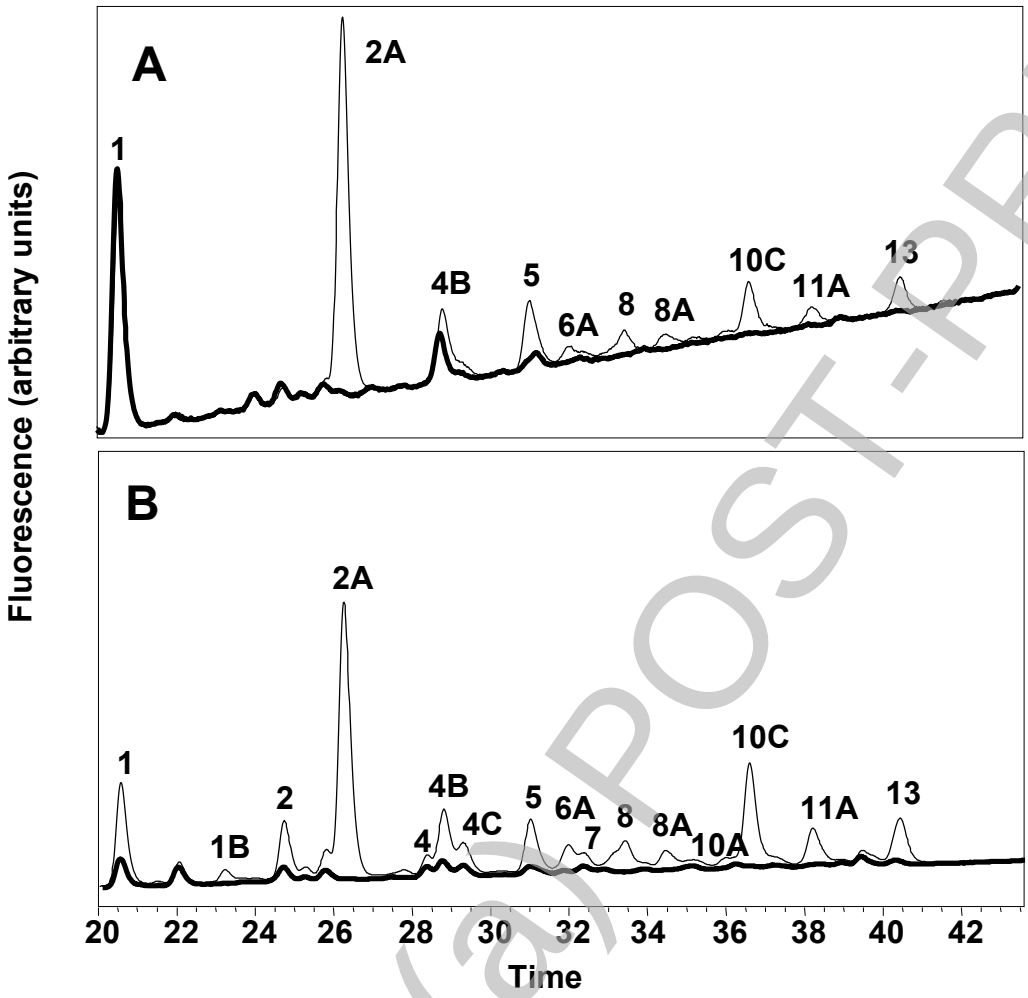

Figure 6

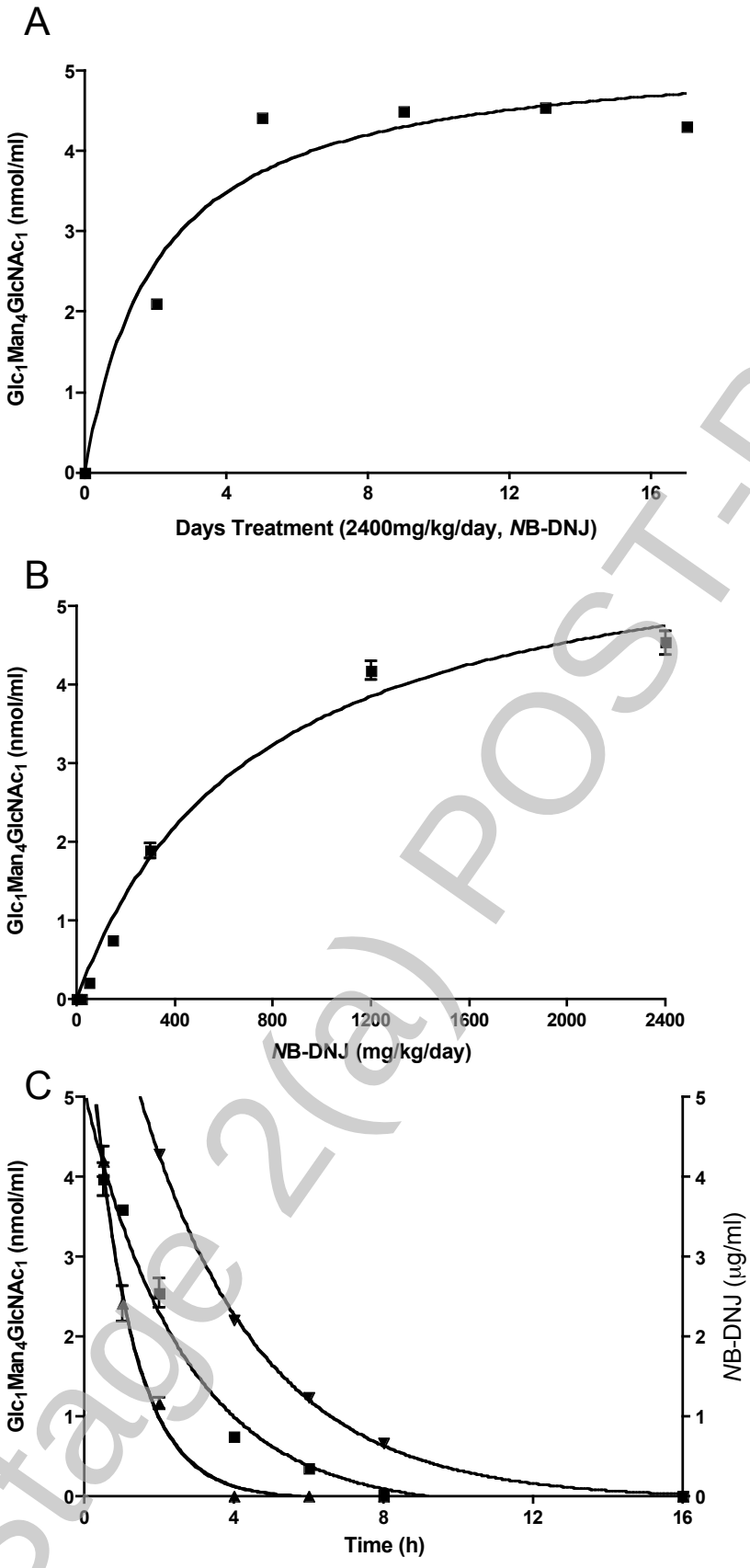

Figure 7

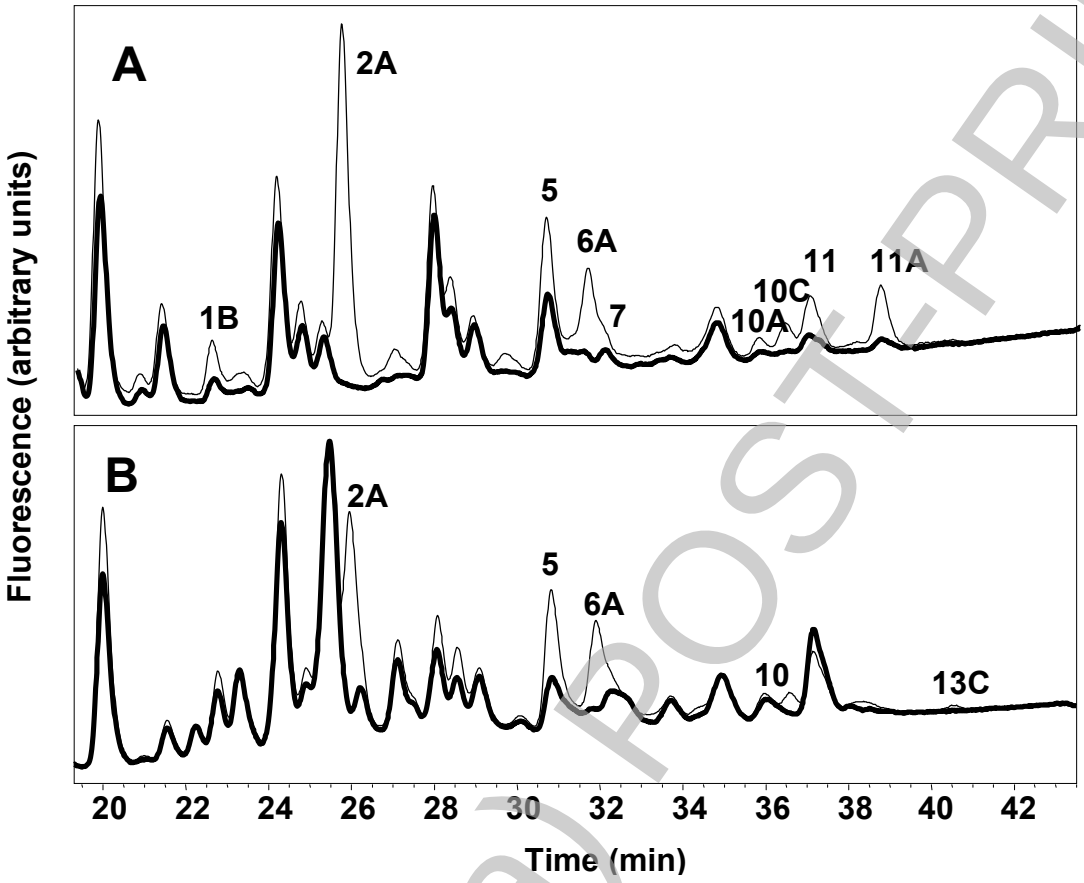

Isolated peak number	Glucose unit	Structure	% in control cells	% in treated cells	Notes
1	3.98	$Man_3GlcNAc_1$	1.07 ± 0.21	0.24 ± 0.01	core
1A	4.14	Contaminant	-	0.41 ± 0.02	
1B	4.56	$Man_4GlcNAc_1$	-	0.09 ± 0.01	linear
2	4.87	$Man_4GlcNAc_1$	14.9 ± 2.61	3.93 ± 0.30	
2A	5.15/5.29	$Man_5GlcNAc_1$/ $Glc_1Man_4GlcNAc_1$	-	0.17 ± 0.01/ 1.05 ± 0.09	
3	5.66	$Man_5GlcNAc_1$	0.55 ± 0.02	0.59 ± 0.02	
4	5.82	$Man_5GlcNAc_1$	50.81 ± 4.9	5.96 ± 1.20	
4A	6.40	Contaminant	-	0.44 ± 0.01	
4B*	5.88	$Man_5GlcNAc_2$	-	-	
4C*	5.99	$Man_5GlcNAc_2$	-	-	
4D*	6.12	$Glc_2Man_4GlcNAc_1$	-	-	
5	6.58	$Glc_1Man_5GlcNAc_1$	16.09 ± 3.8	8.67 ± 1.45	
6	6.81	$Man_6GlcNAc_1$	1.09 ± 0.42	-	
6A*	6.93	$Glc_3Man_4GlcNAc_1$	-	-	
7	6.99	$Man_6GlcNAc_1$/ $Man_6GlcNAc_2$	0.77 ± 0.05	1.56 ± 0.15/ 1.84 ± 0.19	
8	7.29	$Glc_2Man_5GlcNAc_1$/ $Man_7GlcNAc_1$	0.58 ± 0.02/ 0.91± 0.03	5.07 ± 0.47/ -	
8A	7.74	$Man_7GlcNAc_1$	-	0.85 ± 0.03	
9	7.87/7.74	$Man_7GlcNAc_2$/ $Man_7GlcNAc_1$/ $Glc_2Man_6GlcNAc_1$	0.67 ± 0.2/ 0.60 ± 0.01/ -	1.19 ± 0.27/ -/ 0.3 ± 0.02	
10	8.45/8.39/8.29	$Man_8GlcNAc_2$/ $Man_8GlcNAc_1$/ $Glc_3Man_5GlcNAc_1$	0.61 ± 0.02/ 0.20 ± 0.01/ 0.29 ± 0.01	-	
10A	8.23	$Glc_3Man_5GlcNAc_1$	-	34.0 ± 3.6	
10B	8.54	$Glc_1Man_7GlcNAc_1$	-	4.26 ± 0.79	D2 and D3 missing
10C*	8.56	$Glc_1Man_7GlcNAc_2$	-	-	
11	8.78	$Man_8GlcNAc_2$/ $Man_8GlcNAc_1$/	1.58 ± 0.40/ 1.27 ±0.15	0.85 ± 0.17/ 0.69 ± 0.08	
11A	9.07	$Glc_3Man_6GlcNAc_1$/ $Glc_2Man_7GlcNAc_1$	-	1.43 ± 0.3 / 0.92 ± 0.42	
12	9.39	$Man_9GlcNAc_2$/ $Man_9GlcNAc_1$/	3.09 ± 0.5/ 2.52 ± 0.42	-	
12A	9.45	$Glc_3Man_6GlcNAc_1$/ $Glc_1Man_8GlcNAc_1$	-	1.35 ± 0.14 / 0.58 ± 0.06	
12B	9.71	$Glc_3Man_7GlcNAc_1$/ $Glc_3Man_7GlcNAc_2$ / $Glc_1Man_9GlcNAc_1$	-	2.11 ± 0.13/ 0.22 ± 0.01/ 0.22 ± 0.01	D2 and A missing
13	10.14	$Glc_3Man_7GlcNAc_2$/ $Glc_1Man_9GlcNAc_1$	0.06 ± 0.01/ 0.25 ± 0.06	6.02 ± 1.2/ 0.82 ± 0.02	D2 and D3 missing
13A	10.81	$Glc_3Man_8GlcNAc_1$/ $Glc_3Man_8GlcNAc_2$	-	3.86 ± 0.45	D3 missing
13B	11.14	$Glc_3Man_8GlcNAc_1$ / $Glc_3Man_8GlcNAc_2$	-	4.65 ± 0.56	D2 missing
14	11.74	$Glc_3Man_9GlcNAc_2$ / $Glc_3Man_9GlcNAc_1$	0.39 ± 0.01/-	5.00 ± 0.86/ 0.9 ± 0.02	

Table 1: FOS in HL60 cells following treatment with *N*B-DNJ.

Structures, glucose units (GU) values and proportions of FOS isolated peaks produced in HL60 cells (A) in control cells and (B) following treatment with 1 mM *N*B-DNJ for 24 h. The numbers of the isolated peak corresponds to the numbers in Figure 1. The nomenclature shown in the notes refers to the structure below. The mean value from three experiments is shown ± SD.

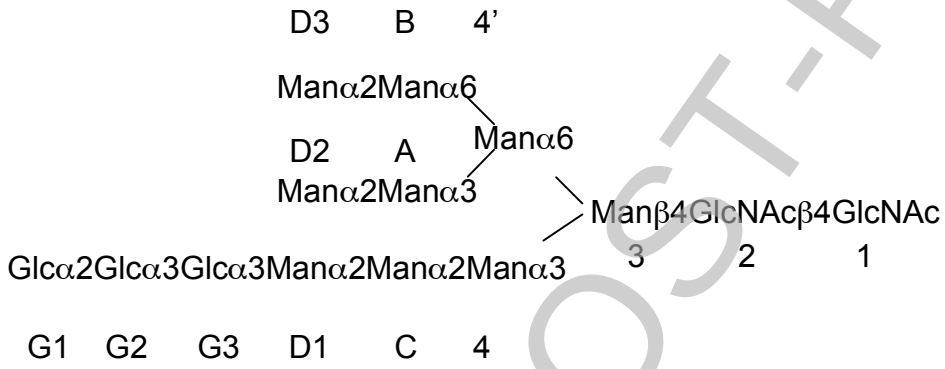

* FOS structures observed in mouse tissue, serum and urine, and human plasma and urine, see Figs 4, 5 and 7

Substrate	Enzyme	IC_{50} (μM)
$Glc_3Man_9GlcNAc_2$	α-glucosidase I	0.59 ± 0.08
$Glc_3Man_5GlcNAc_1$	α-glucosidase I	0.68 ± 0.15
$Glc_2Man_5GlcNAc_1$	α-glucosidase II	10.8 ± 1.13
$Glc_1Man_5GlcNAc_1$	α-glucosidase II	53.0 ± 16.6

Table 2. In vitro inhibition of α-glucosidases by *N*B-DNJ.

2-AA labelled substrates for purified glucosidases I and II were purified by preparative HPLC and incubated in the presence of enzyme and various concentrations of *N*B-DNJ. Separation of the reaction products by NP-HPLC and measurement of peak areas was used to quantify the amount of hydrolysis to derive IC_{50} values as shown. The experiment was performed in triplicate and the mean ± SD is shown.

Mouse Tissue/Sample	Total FOS (pmol/mg)	
	- *N*B-DNJ	+ *N*B-DNJ
Heart	5.4 ± 0.1	12.6 ± 5.0
Kidney	16.8 ± 3.9	52.9 ± 21.0
Lung	12.0 ± 0.6	28.9 ± 3.6
Liver	29.4 ± 5.8	86.2 ± 12.4
Brain	3.2 ± 0.2	5.4 ± 1.0
Spleen	4.1 ± 0.7	7.2 ± 2.3
	Total FOS (nmol/ml)	
	- *N*B-DNJ	+ *N*B-DNJ
Serum	5.76 ± 0.8	12.4 ± 2.6
Urine	10.6 ± 3.6	31.9 ± 7.2

Table 3. FOS in murine tissues, serum and urine following treatment with *N*B-DNJ.

Total amounts of FOS, pmol/mg (wet weight) in tissue samples and nmol/ml in serum and urine were calculated from peak areas of all high-mannose oligosaccharide species containing greater than three mannose residues having one or more core N-acetylglucosamine residues after analytical separation by NP-HPLC. The mean value from five animals per group is shown ± SD. The increase in FOS in all tissues was significant at the 95% confidence level using Student's t-Test.